

Quantifying the Effects of Ischaemia on Electrophysiology and the ST Segment of the ECG in Human Virtual Ventricular Cells and Tissues

AP Benson^{1,2}, EK Hodgson¹, O Bernus^{1,2}, AV Holden^{1,2}

¹Institute of Membrane and Systems Biology, University of Leeds, Leeds, UK

²Multidisciplinary Cardiovascular Research Centre, University of Leeds, Leeds, UK

Abstract

We have developed human virtual cell and tissue models of ischaemia, and used these models to quantify electrophysiological and ECG ST segment changes during sub-endocardial and global ischaemia. Our investigation has highlighted key differences with previous computational studies based on animal models: (i) propagation failure in the human model occurs with a smaller degree of hyperkalaemia compared to previously used animal models, due to differences in sodium channels kinetics; (ii) the human model is more sensitive to repolarising potassium currents during phase 3 repolarisation than the previously used animal models, and therefore the magnitude of the ATP-sensitive potassium current must be smaller in the human model to produce similar changes in action potential duration during ischaemia; and (iii) unlike in animal models where hyperkalaemia was identified as the major component of ST segment depression, we find in the human model that both anoxia and hyperkalaemia are responsible.

1. Introduction

Myocardial ischaemia is caused by reduced coronary blood flow and can lead to critical impairment of both the electrical and mechanical functioning of the heart [1]. In Europe, ischaemic heart disease accounts for nearly two million deaths per year [2]. Measuring changes in an electrocardiogram (ECG), particularly ST segment depression or elevation, can yield useful clinical information to enable the extent of ischaemia to be determined – this is the most commonly used method in patients with suspected ischaemic heart disease [3]. However, it is often difficult to identify the underlying electrophysiological mechanisms of ST segment changes in a clinical setting. Computer simulations using virtual cells and tissues help overcome some of the limitations of clinical studies, as they are able

to dissect out and examine the relationships between individual electrophysiological parameters. Previous work in our laboratory [4] has examined mechanisms of ECG changes during ischaemia using a computational model of guinea pig tissue, and identified both dynamic and static electrophysiological mechanisms that are responsible for changes to the ECG ST segment. Hyperkalaemia was found to be the major contributor to both these mechanisms. However, it is unclear whether the mechanisms identified in the guinea pig model will be pertinent in human ischaemia. We have therefore developed human virtual cell and tissue models of ischaemia, and used these models to quantify electrophysiological and ECG changes during sub-endocardial and global ischaemia.

2. Methods

For a single isopotential cell, the rate of change of membrane potential V is given by

$$\frac{dV}{dt} = -I_{\text{ion}} \quad (1)$$

where t is time and I_{ion} is the total membrane ionic current density, given here by the human model of Ten Tusscher & Panfilov [5] which includes parameters for endocardial, midmyocardial and epicardial cells. Parameter changes were made to simulate the individual component changes seen during ischaemia – hyperkalaemia, acidosis and anoxia – as in Shaw & Rudy [6], but with extracellular potassium during hyperkalaemia set to $[\text{K}^+]_{\text{o}} = 10 \text{ mM}$ and with an 80% reduction in the maximal conductance of the ATP-sensitive K^+ current $I_{\text{K(ATP)}}$ to ensure realistic changes in resting membrane potential and action potential duration (APD) respectively (see Results).

These cell models were incorporated into a heterogeneous 15 mm one-dimensional strand model of the human left ventricular wall [7]. Propagation of electrical excita-

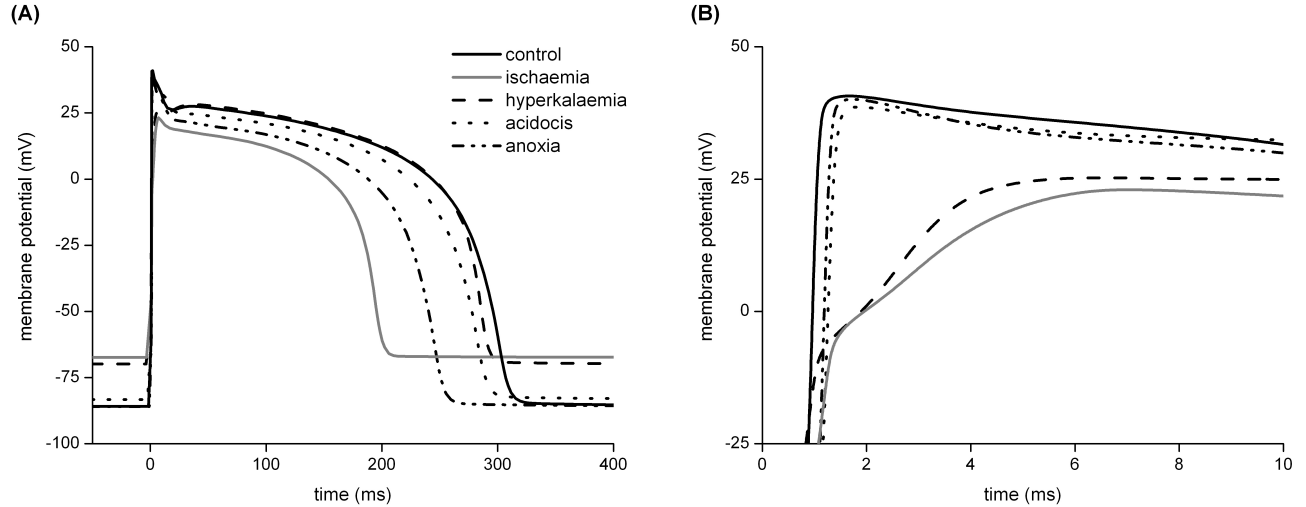


Figure 1. (A) Computed steady state (1 Hz pacing) action potentials in control (black solid line) and ischaemic (grey solid line) endocardial cells. Also shown are action potentials for endocardial cells in which only a single component part of ischaemia is included. (B) Magnification of panel A, showing the second half of phase 0 depolarisation and the reduced upstroke velocity and phase 0 amplitude in the hyperkalaemic and ischaemic cells.

Table 1. Action potential duration (APD) measured at 1 Hz pacing in endocardial, midmyocardial and epicardial human cell models. Shown are values for control and ischaemic cells, plus cells with the component parts of ischaemia in isolation, and the change in APD (Δ APD) with respect to control.

	Endocardial		Midmyocardial		Epicardial	
	APD (ms)	Δ APD (%)	APD (ms)	Δ APD (%)	APD (ms)	Δ APD (%)
Control	307		414		308	
Hyperkalaemia	293	-5	391	-6	294	-5
Acidosis	288	-6	381	-8	289	-6
Anoxia	249	-19	296	-29	247	-20
Ischaemia	203	-34	233	-44	201	-35

tion in such a model of cardiac tissue is described by

$$\frac{\partial V}{\partial t} = D(\nabla^2 V) - I_{\text{ion}} . \quad (2)$$

Here, $D = 0.154 \text{ mm}^2 \text{ ms}^{-1}$ is a diffusion coefficient that characterises electrotonic spread of voltage through the tissue, and $\nabla \equiv \partial/\partial x$ is a spatial gradient operator. We set the spatial distribution of endocardial, midmyocardial and epicardial tissue types using the ratio 3:5:7 in order that an upright ECG T wave was produced under control (non-ischaemic) conditions, and set the transmural values of $I_{K(\text{ATP})}$ half-maximal saturation as in [8]. The ECG was represented by the ventricular electrogram (the pseudo-ECG), computed using

$$\Phi = \frac{a^2}{4} \int (-\nabla V) \left(\nabla \frac{1}{x-x'} \right) dx , \quad (3)$$

where Φ represents the unipolar potential recorded at an electrode 2 cm from the epicardial end of the strand, a is

the radius of the fibre and $x - x'$ is the distance from the electrode to any point in the tissue [9]. Integration details for the models can be found in [7].

3. Results

Figure 1 shows action potentials recorded from single endocardial human cell models at 1 Hz pacing, for control and ischaemic conditions plus the component parts of ischaemia in isolation.

Hyperkalaemia (dashed line in Figure 1A) caused the greatest depolarisation of resting membrane potential, from -86 mV in control cells with $[\text{K}^+]_o = 5.4 \text{ mM}$ to -70 mV with $[\text{K}^+]_o = 10 \text{ mM}$. Note that we did not use the hyperkalaemic value of $[\text{K}^+]_o = 12 \text{ mM}$ as used in a guinea pig model [6] as such a degree of hyperkalaemia in the human model resulted in conduction block when simulating propagation in the tissue. Such propagation block occurred because relatively more sodium (Na^+) channels

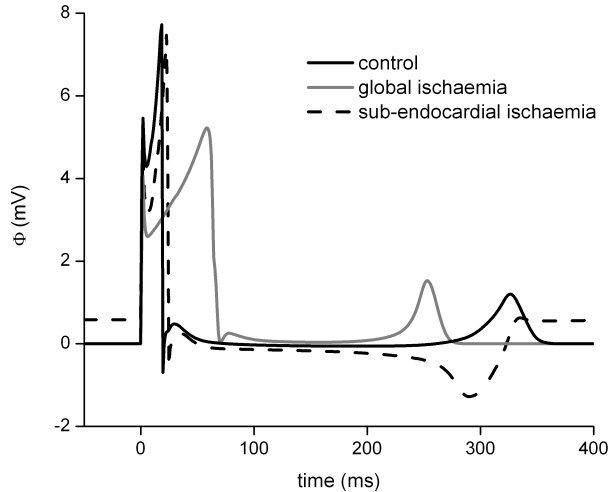


Figure 2. Steady state pseudo-ECGs recorded from control (black solid line), globally ischaemic (grey solid line) and sub-endocardially ischaemic (dashed black line) tissue models at 1 Hz pacing. In this instance, sub-endocardial ischaemia is with 3 mm of ischaemic tissue at the endocardial end of the 15 mm tissue strand.

remain in the inactivated state due to a negative shift in the inactivation curve of the human Na^+ current I_{Na} compared to the guinea pig model (see Figure 1B in reference [10]). Acidosis caused a 3 mV depolarisation of resting membrane potential, while anoxia had virtually no effect. The effects of the three components were additive, as the ischaemic resting membrane potential was -67 mV. Any depolarisation of the resting membrane potential will result in some Na^+ channels remaining inactivated (although with the parameters used in our human models, there are enough available channels for depolarisation and propagation to occur) and a concomitant reduction in membrane excitability. This reduced excitability can be seen in the reduced phase 0 upstroke velocity and phase 0 magnitude of the hyperkalaemic and ischaemic action potentials in Figure 1B, and the wider QRS complex in the ischaemic ECGs shown in Figure 2, which are due to slower conduction along the tissue strand.

The anoxic component of ischaemia (dash-dot line in Figure 1A) caused the greatest shortening of APD – from 307 ms in control cells to 249 ms, a reduction of 19% – and as such is the greatest contributor to abnormal repolarisation patterns. Hyperkalaemia and acidosis caused 5% and 6% reductions in APD respectively. Ischaemia resulted in a 34% reduction of APD to 203 ms, and so the net effects of the three components of ischaemia on APD shortening are roughly additive. Qualitatively similar results were found in the midmyocardial and epicardial cell models (see Table 1). Note that, for the human models, we used a value for the maximal conductance of $I_{\text{K(ATP)}}$ (active during anoxia

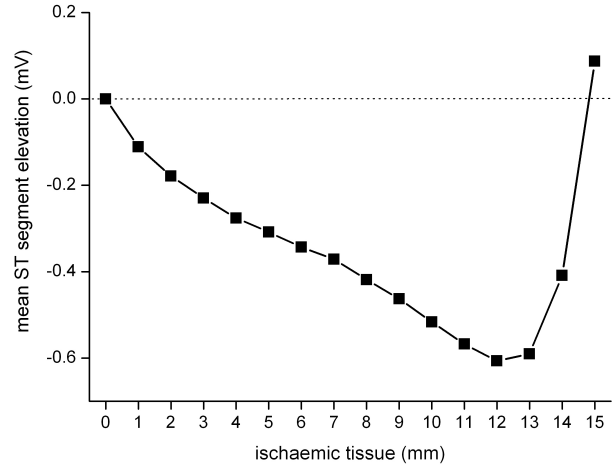


Figure 3. Mean ST segment elevation with respect to baseline, for varying degrees of sub-endocardial ischaemia. The abscissa indicates the length of the ischaemic tissue, from the endocardial end of the strand. Note that 15 mm of ischaemic tissue corresponds to global ischaemia.

and ischaemia) that was only 20% of the value in a previously used guinea pig model [6] in order to produce similar reductions in APD, as the human model is much more sensitive to repolarising currents during phase 3 repolarisation. We therefore hypothesise that any such current recorded experimentally from human tissue will be much smaller than the equivalent current recorded from guinea pig tissue.

Figure 2 shows ECGs recorded from the human tissue model (1 Hz pacing from the endocardial end of the strand). The control tissue gave a flat, neutral ST segment and an upright T wave due to the asymmetrical distribution of tissue types. Global ischaemia (i.e. with the entire strand ischaemic) caused a widening of the QRS complex due to reduced tissue excitability, and a shortening of the ST segment due to reduced APD. There was slight elevation of the ST segment, but no change to the baseline. Sub-endocardial ischaemia – in this case with 3 mm of the 15 mm strand (i.e. the entire endocardial region) ischaemic – caused elevation of the baseline ECG compared to control, widening of the QRS complex, a depression in the ST segment and an inverted T wave. Aslanidi *et al.* [4], using a guinea pig tissue model, identified two spatial gradients responsible for ST segment depression during sub-endocardial ischaemia: “static” gradients due to differences in resting membrane potential between ischaemic and non-ischaemic tissue, and “dynamic” gradients due to an abnormal repolarisation sequence which they attributed to changes in APD. They concluded that hyperkalaemia was the underlying electrophysiological mechanism responsible for both gradients. In the human tissue model we

find that, although gradients in resting membrane potential are due to hyperkalaemia, the component mainly responsible for changes to APD, and therefore abnormal repolarisation patterns, is anoxia (see Figure 1 and Table 1). Thus, we conclude that the static and dynamic gradients responsible for ST segment depression during sub-endocardial ischaemia in the human model are due to hyperkalaemia and anoxia respectively.

Figure 3 shows the degree of ST segment depression in the human strand model for varying spatial extents of sub-endocardial ischaemia. With ischaemic regions between 1 mm and 12 mm in length, the degree of ST segment depression increases monotonically. Maximum ST segment depression is found with 12 mm of the 15 mm strand ischaemic. With global ischaemia, there is slight ST segment elevation. This pattern of depression and elevation is similar to that previously reported using a guinea pig model [4].

4. Discussion and conclusions

We have developed an electrophysiological model of ischaemia in human ventricular myocardium, and performed the first mechanistic investigation of ST segment depression in such a model. We have highlighted key differences with previous computational studies based on animal models, namely: (i) propagation failure in the human model occurred with a smaller degree of hyperkalaemia (with $[K^+]_o > 10$ mM) compared to previously used animal models. This is due to differences in Na^+ channels kinetics; (ii) the human model is more sensitive to repolarising K^+ currents during phase 3 repolarisation than the previously used animal models. As such, the magnitude of $I_{K(ATP)}$ must be smaller in the human model to produce similar changes in APD; and (iii) unlike Aslanidi *et al.* [4] who identified hyperkalaemia as the main contributor to ST segment depression using an animal model, we found in the human model that the main contributors are both anoxia and hyperkalaemia.

Acknowledgements

This work was supported by the Dr Hadwen Trust for Humane Research, and the European Union through the BioSim Network of Excellence (contract number LSHB-CT-2004-005137).

References

- [1] Carmeliet E. Cardiac ionic currents and acute ischemia: from channels to arrhythmias. *Physiol Rev* 1999;79:917–1017.
- [2] Falk E, Prediman KS, de Feyter PJ. *Ischemic Heart Disease*. London: Manson, 2007.
- [3] Channer K, Morris F. ABC of clinical electrocardiology: myocardial ischaemia. *Brit Med J* 2002;324:1023–26.
- [4] Aslanidi OV, Clayton RH, Lambert JL, Holden AV. Dynamical and cellular electrophysiological mechanisms of ECG changes during ischaemia. *J Theor Biol* 2005;237:369–81.
- [5] Ten Tusscher KHWJ, Panfilov AV. Alternans and spiral breakup in a human ventricular tissue model. *Am J Physiol* 2006;291:H1088–100.
- [6] Shaw RM, Rudy Y. Electrophysiologic effects of acute myocardial ischaemia: a theoretical study of altered cell excitability and action potential duration. *Cardiovasc Res* 1997;35:256–72.
- [7] Benson AP, Halley G, Li P, Tong WC, Holden AV. Virtual cell and tissue dynamics of ectopic activation of the ventricles. *Chaos* 2007;17:015105.
- [8] Gima K, Rudy Y. Ionic current basis of electrocardiographic waveforms: a model study. *Circ Res* 2002;90:889–96.
- [9] Plonsey R, Barr RC. *Bioelectricity: A Quantitative Approach*. New York: Plenum Press, 1988.
- [10] Ten Tusscher KHWJ, Noble D, Noble PJ, Panfilov AV. A model for human ventricular tissue. *Am J Physiol* 2004;286:H1573–89.

Address for correspondence:

Alan Benson
Institute of Membrane and Systems Biology
Garstang Building
University of Leeds
Leeds LS2 9JT
UK
a.p.benson@leeds.ac.uk